Child's Nervous System (2019) 35:119–128
https://doi.org/10.1007/s00381-018-3870-2

ORIGINAL PAPER

# Surgical histopathology of limited dorsal myeloschisis with flat skin lesion

Takato Morioka[1] · Satoshi O. Suzuki[2] · Nobuya Murakami[1] · Nobutaka Mukae[3] · Takafumi Shimogawa[1,3] · Hironori Haruyama[3] · Ryutaro Kira[4] · Koji Iihara[3]

Received: 26 April 2018 / Accepted: 15 June 2018 / Published online: 22 June 2018


## Abstract

**Purpose** Limited dorsal myeloschisis (LDM) is characterized by two invariable features: a focal *closed* neural tube defect and a fibroneural stalk linking the skin lesion to the underlying spinal cord. Although detailed histopathological findings of the LDM stalk were originally described by Pang et al., the precise relationship between the histopathological findings and clinical manifestations including intraoperative findings has not been fully determined.

**Methods** We retrospectively analyzed the histopathological findings of the almost entire stalk and their relevance to the clinical manifestations in six Japanese LDM patients with flat skin lesions.

**Results** Glial fibrillary acidic protein (GFAP)-immunopositive neuroglial tissues were observed in three of the six patients. Unlike neuroglial tissues, peripheral nerve fibers were observed in every stalk. In four patients, dermal melanocytosis, "Mongolian spot," was seen surrounding the cigarette-burn lesion. In three of these four patients, numerous melanocytes were distributed linearly along the long axis of the LDM stalk, which might represent migration of melanocytes from trunk neural crest cells during formation of the LDM stalk.

**Conclusion** Immunopositivity for GFAP in the LDM stalk was observed in as few as 50% of our patients, despite the relatively extensive histopathological examination. We confirm that the clinical diagnosis of LDM should be made based on comprehensive histopathological examination as well as clinical manifestations. The profuse network of peripheral nerve fibers in every stalk and the high incidence of melanocyte accumulation associated with dermal melanocytosis might assist the histopathological diagnosis of LDM.

**Keywords** Glial fibrillary acidic protein · Peripheral nerves · Melanocyte · Untethering

## Introduction

Limited dorsal myeloschisis (LDM) was first described as a distinct clinicopathological entity by Pang et al. in 2010 [16].

LDMs are characterized by two invariable features: a focal *closed* neural tube defect and a fibroneural stalk linking the skin lesion to the underlying spinal cord [16, 17]. The embryogenesis of LDM is hypothesized to be incomplete disjunction between cutaneous and neural ectoderms, which prevents complete midline skin closure and allows a persistent fibroneural stalk between the disjunction site and the dorsal neural tube [16, 17]. LDMs are categorized based on their external skin manifestations as saccular and nonsaccular (flat) [16, 17]. Saccular LDM consists of a skin-based cerebrospinal fluid sac topped by a squamous epithelial dome; flat LDM has a squamous epithelial flat surface or sunken crater or pit, typically called a "cigarette-burn" skin lesion [11]. The fibroneural stalks of nonsaccular LDMs vary in thickness and complexity. In all LDMs, the fibroneural stalk is tethered to the cord, and recommended treatment consists of untethering the stalk from the cord [16, 17].

✉ Takato Morioka
takato@ns.med.kyushu-u.ac.jp

[1] Department of Neurosurgery, Fukuoka Children's Hospital, 5-1-1 Kashii-teriha, Higashi-ku, Fukuoka 813-0017, Japan

[2] Department of Neuropathology, Graduate School of Medical Sciences, Kyushu University, Fukuoka, Japan

[3] Department of Neurosurgery, Graduate School of Medical Sciences, Kyushu University, Fukuoka, Japan

[4] Department of Pediatric Neurology, Fukuoka Children's Hospital, Fukuoka, Japan

**Table 1** Clinical and histopathological findings of six patients with limited dorsal myeloschisis with flat skin lesion

| Patient No. | Age Gender | Hyperpigmented skin[b] | Myofascial entry<br>Dural entry<br>Joining the cord | Tissues in the fibrocollagenous stalk | | | Associated anomaly |
|---|---|---|---|---|---|---|---|
| | | | | Skin-subcutaneous tissue | Extradural stalk | Intradural stalk | |
| 1 | 4 m<br>M | + | L5<br>L3<br>L1–2 | Melanocytes, fat | Peripheral nerves, melanocytes | GFAP, peripheral nerves, melanocytes | |
| 2[a] | 3 m<br>M | + | L5–S1<br>L4–5<br>L3 | Peripheral nerves, melanocytes | Peripheral nerves, melanocytes | Peripheral nerves, melanocytes | |
| 3[a] | 5 m<br>M | + | S1–S2<br>L4<br>L3 | GFAP, melanocytes, fat, Pacinian corpuscles | Peripheral nerves, melanocytes, fat | Peripheral nerves, melanocytes, fat, skeletal muscle | Caudal-type lipoma |
| 4[a] | 5 y<br>F | – | S1–2<br>S1–2<br>L4 | Fat, various ectopic tissues[c] | Peripheral nerves, smooth muscle | Peripheral nerves, ganglion, cartilage | Type-II SCM, neurenteric cyst |
| 5 | 2 y 6 m<br>F | – | S1–2<br>S1<br>L3 | Fat | Peripheral nerves, fat | GFAP, fat | Filar-type lipoma |
| 6 | 3 m<br>F | + | S2<br>L5<br>L3–4 | Melanocytes, fat | | Peripheral nerves | |

*m* month, *y* year, *F* female, *M* male, *Fat* fatty adipose tissue, *GFAP* glial fibrillary acidic protein-immunopositive glial tissue, *SCM* split cord malformation

[a] Patients 2, 3, and 4 in this study were partly reported as cases 2, 3, and 4, respectively, in our previous report [11]

[b] Hyperpigmented skin (Mongolian spot), surrounding the cigarette-burning skin lesion

[c] Lymph follicles, a cartilage island, a cavity lined by transitional epithelium, sebaceous glands, apocrine and eccrine seat glands, Pacinian corpuscles, smooth muscle fibers, ganglion cells, and arachnoid epithelium

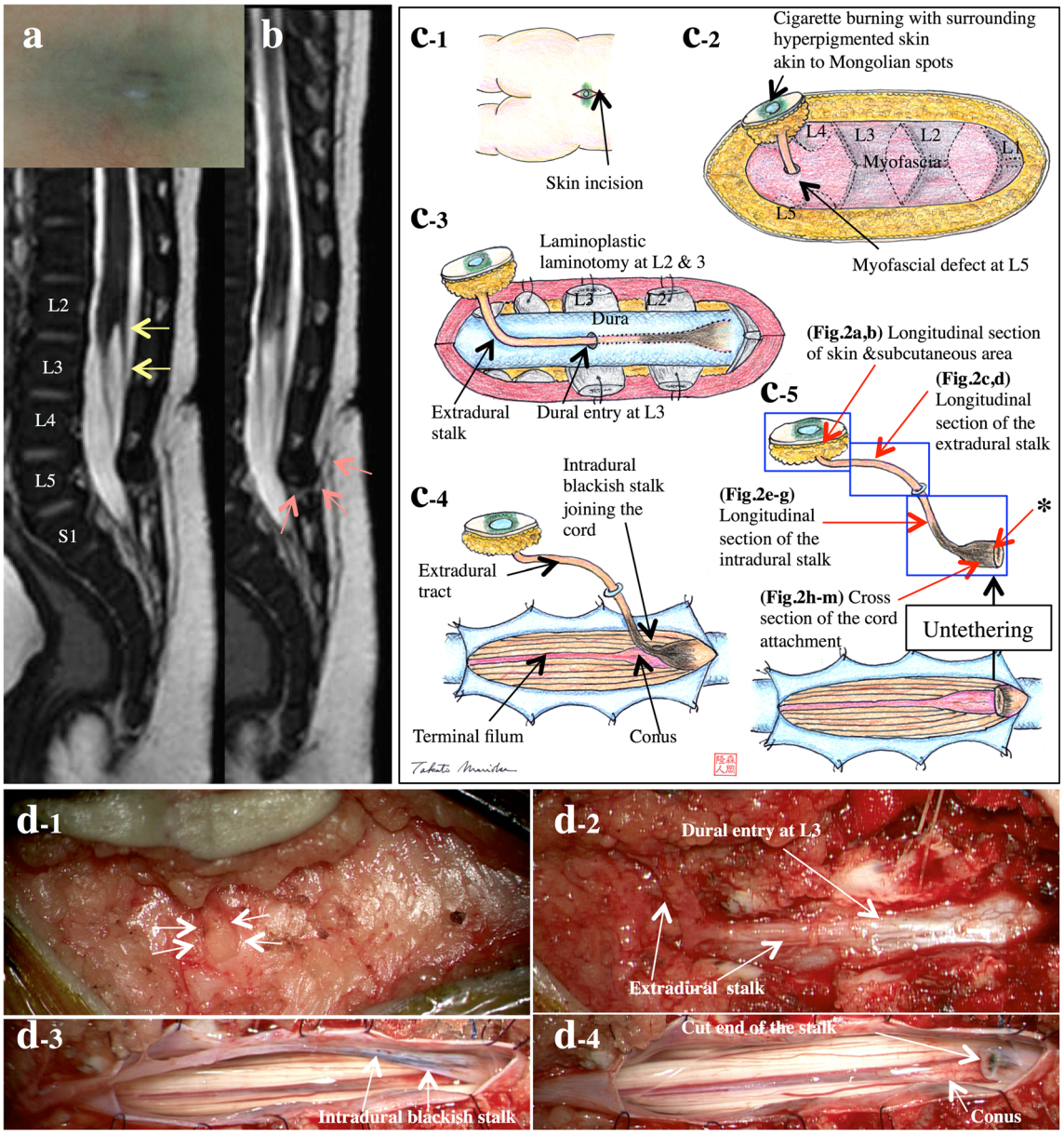


**Fig. 1** Patient 1 (with glial fibrillary acidic protein (GFAP)-immunopositive neuroglial tissues and high numbers of melanocytes containing stalk). (*a*) Photograph showing a cigarette-burn skin lesion with surrounding hyperpigmented skin, "Mongolian spot." (*b*) Serial sagittal views of three-dimensional heavily T2-weighted images (3D-hT2WI) showing an isointense subcutaneous (red arrows) and intraspinal stalk (yellow arrows) passing through the spinal canal opposite L5 and joining the conus at L1–2. (*c*) Schematic drawing and (*d*) microscopic view of the operative findings. The small-diameter stalk starts at the subcutaneous fat, passes through the fascia at the level of the bifid L5 (*c-1*, *c-2*, *d-1* white arrows), runs epidurally, and enters intradurally at the L3 level (*c-3*, *d-2*). Upon opening the dura, the blackish intradural stalk (*c-4*, *d-3*) joins the dorsal surface of the cord above the conus (*c-4*, *d-3*). Once the intradural stalk is disconnected from the cord to untether the cord (*c-5*), en bloc resection of the entire stalk is performed (*c-5*, *d-4*). The center of the cut end of the stalk is black-colored (*c-5*, *d-4*). The entire tract is divided into three parts (skin and subcutaneous tissue, extradural stalk, and intradural stalk) (*c-5*, blue squares) and submitted for histological examination

When diagnosing LDM with flat skin lesions, histopathological confirmation of the neuroglial tissue in the fibrocollagenous stalk, as a hallmark of the stalk's origin from nondisjoined neuroectoderm, is important [16, 17], and immunohistochemical detection of glial fibrillary acidic protein (GFAP)-expressing tissue is commonly used [7, 11, 16, 17].

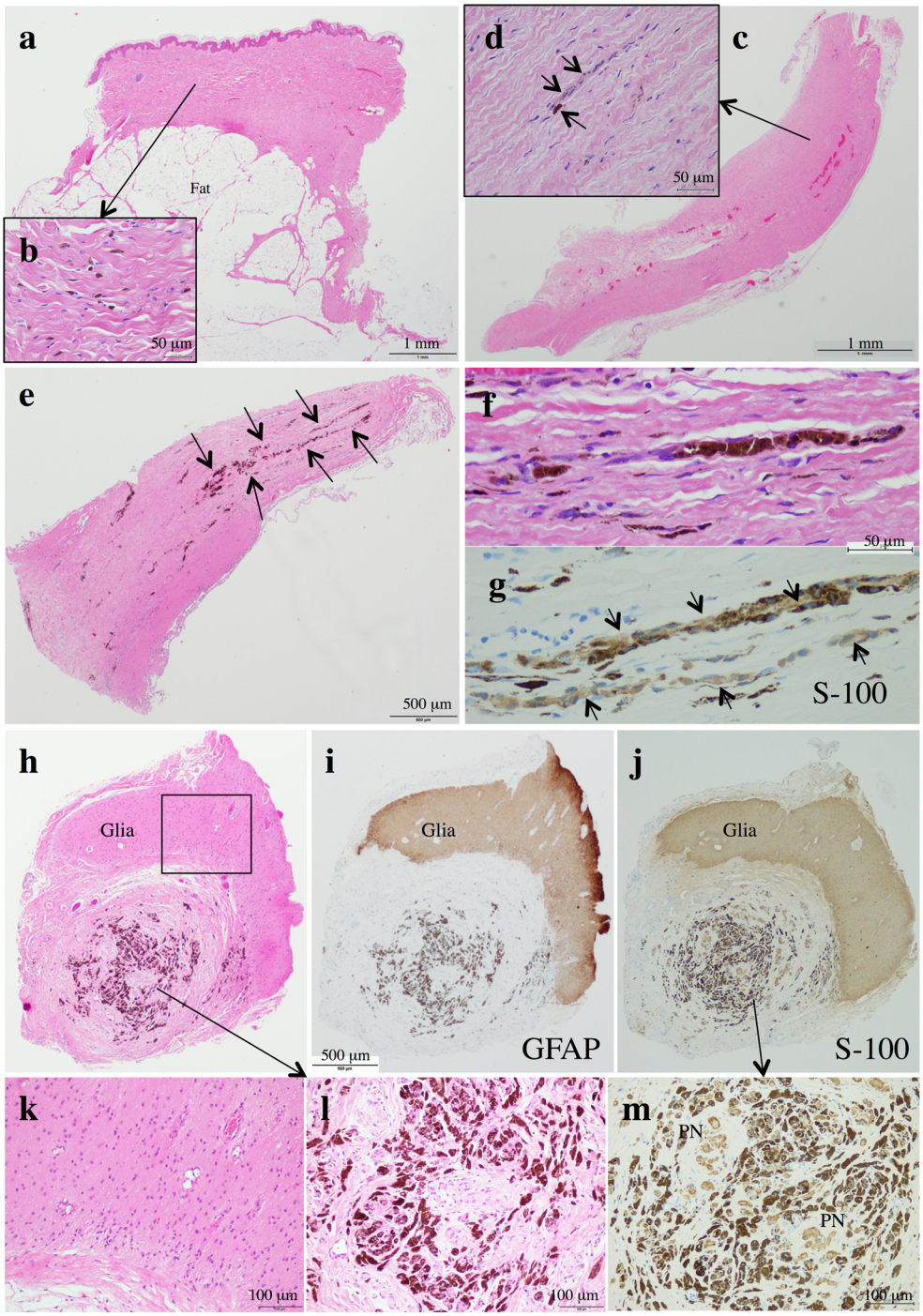


**Fig. 2** Patient 1. Histopathological findings of the stalk. Each section is indicated in Fig. 1c-5. (*a*) Skin tissue with finely jagged squamous epithelium continues to the subcutaneous mature adipose tissue (fat) with loose connective tissue. (*b*) High-power field view of the dermis showing an increased number of dermal melanocytes. (*c*) Extradural stalk showing the fibrocollagenous tract. (*d*) High-power field view of the extradural stalk showing a number of melanocytes distributed along the collagenous fibers (black arrows). (*e*, *f*) Intradural stalk showing numerous melanocytes distributed linearly along the long axis of the fibrocollagenous tract (black arrows). (*f*) High-power view of the intradural tract. (*g*) High-power view of the intradural tract with immunostaining for S-100 protein (S-100) showing melanocytes (stained in dark brown) distributed along the peripheral nerve fibers (stained in light brown, black arrows). (*h*–*m*) Cross section of the intradural tract near the attachment to the cord with hematoxylin and eosin staining (*h*, *k*, *l*) and immunostaining for GFAP (*i*) and S-100 (*j*, *m*) showing GFAP-immunopositive neuroglial tissue (Glia) surrounding one-half of the fibrocollagenous bundle and which contains numerous melanocytes and peripheral nerve fibers (PN, stained in light brown with immunostaining for S-100 in (*m*)). (*k*) High-power field view of the area indicated by the open square in (*h*). (*l*, *m*) High-power views of (*h*) and (*j*), respectively. The position of the GFAP-immunopositive neuroglial tissues is indicated by a black asterisk in Fig. 1c-5

However, recent reports [7, 8, 11] demonstrated that GFAP-immunopositive neuroglial tissue is not noted in every stalk; therefore, the diagnosis of LDM should be based on comprehensive evaluation of histopathological findings as well as clinical manifestations [11]. Detailed histopathological findings in the LDM stalk were originally described by [16, 17]; however, the precise relationship between histopathological findings and clinical manifestations including intraoperative findings has not been fully determined. Although we previously partially reported the neurosurgical pathology of three of our patients with flat LDM lesions [11], a recent additional three cases prompted us to report the detailed histopathological findings as they relate to the clinical manifestations, for all six LDM patients.

## Patients and methods

From July 2015 to March 2018, 67 Japanese patients with a closed neural tube defect underwent initial untethering surgery at Kyushu University Hospital and related hospitals by the first author (TM). Six of the 67 patients (8.96%) were diagnosed with flat LDM lesions based on clinical, neuroradiological, intraoperative, and histopathological findings (Table 1). Patients 2, 3, and 4 in the current study were reported as cases 2, 3, and 4 in our previous report [11], respectively. The median age was 1 year and 5.5 months at operation (range, 3 months to 5 years), and three patients were girls.

All patients had "cigarette-burn" flat skin lesions on the lumbosacral midline (Figs. 1a, 3a, and 4a). Preoperative magnetic resonance imaging (MRI), including three-dimensional T1-weighted spoiled gradient-recalled echo images and three-dimensional heavily T2-weighted images (3D-hT2WI) as well as conventional T1- and T2-weighted images, was performed as described previously [5, 6, 9–11, 13–15, 18]. MR images, especially 3D-hT2WI, demonstrated the pathognomonic isointense stalk connecting the skin lesion to the spinal cord following a discrete extra- and intradural course (Figs. 1b, 3b, c, and 4b). In all patients, the LDM stalk was located in the lumbosacral region.

At surgery in patients 1–4, the stalk was dissected extradurally and then intradurally to the attachment to the cord. Once the intradural stalk was disconnected from the cord, the stalk with its skin lesion was resected en bloc (Fig. 1c, d). In patient 5, the stalk's attachment to the cord was estimated at the level of L3 through laminotomy of L4; we did not perform additional laminotomy of L3 to expose the attachment (Fig. 3d, e). The almost entire tract of patients 1–5 was divided into three parts (skin and subcutaneous tissue, extradural stalk, and intradural stalk) and was submitted for histological examination (Figs. 1c-5 and 3d-6, blue open squares). In patient 6, although the stalk's attachment on the lower-lying cord was confirmed at L4, the most caudal nerve roots were adhered to the ventral side of the LDM stalk (Fig. 4c-1, d-1, d-2). For untethering in patient 6, we resected the most caudal part of the intradural stalk to avoid nerve injury (Fig. 4c-5, d-3, d-4). The most rostral part of the extradural stalk was not resected because the epidural peripheral nerves were adhered (Fig. 4c-5, d-3, d-4). Skin and subcutaneous tissue and the intradural stalk were submitted for histological examination (Fig. 4c-5). We retrospectively analyzed the histopathological findings of the stalk as they related to the clinical manifestations.

## Results

The clinical and histopathological findings of the six patients are summarized in Table 1. Three (patients 1, 3, and 5) of the six patients (50%) had GFAP-immunopositive neuroglial tissues in the fibrocollagenous stalk. In two patients (patients 1 and 5), GFAP-immunopositive neuroglial tissue was observed only caudal to the cord-stalk attachment site of the intradural stalk (Figs. 1c-5*, 2h–k, and 3d-6*, j–l), while in patient 3, a small nest of GFAP-immunopositive neuroglial tissue was embedded in the subcutaneous lipomatous tissue. In all patients, no GFAP-immunopositive neuroglial tissue was observed in the epidural stalk and caudal part of the intradural stalk. We also saw none in large, elongated swaths containing scattered neurons nor any in nests embedded in dense fibrous tissue [16, 17] in our study.

Unlike the neuroglial tissues, peripheral nerve fibers were observed in every stalk in this study. In four patients (patients 1–4), peripheral nerve fibers were noted both in the extra- and intradural stalks (Fig. 2g, j, m). Peripheral nerve fibers were observed in the extradural stalk of patient 5 (Fig. 3i) and the intradural stalk of patient 6 (Fig. 4g).

In four patients (patients 1, 2, 3, and 6), hyperpigmented skin areas, "Mongolian spot," surrounded the cigarette-burn lesion (Figs. 1a and 4a). In these patients, skin tissue had an increased number of dermal melanocytes (dermal melanocytosis) (Figs. 2a, b and 4e, f). In three of these four patients (patients 1, 2, and 3), melanocytes were also observed both in the extra- and intradural stalks (Fig. 2d–j, l, m). Especially in the intradural stalk, numerous melanocytes were distributed linearly along the long axis of the fibrocollagenous stalk (Fig. 2e–g). Melanocyte accumulation was also observed along the S-100 protein (S-100)-immunopositive peripheral nerve fibers (Fig. 2f, g, j, m). Intraoperatively, the intradural stalk containing high numbers of melanocytes was seen as a black color (Fig. 1c-4, c-5, d-3, d-4).

The most frequently observed mesodermal tissue, except for fibrovascular tissues, was fatty adipose tissue, especially in

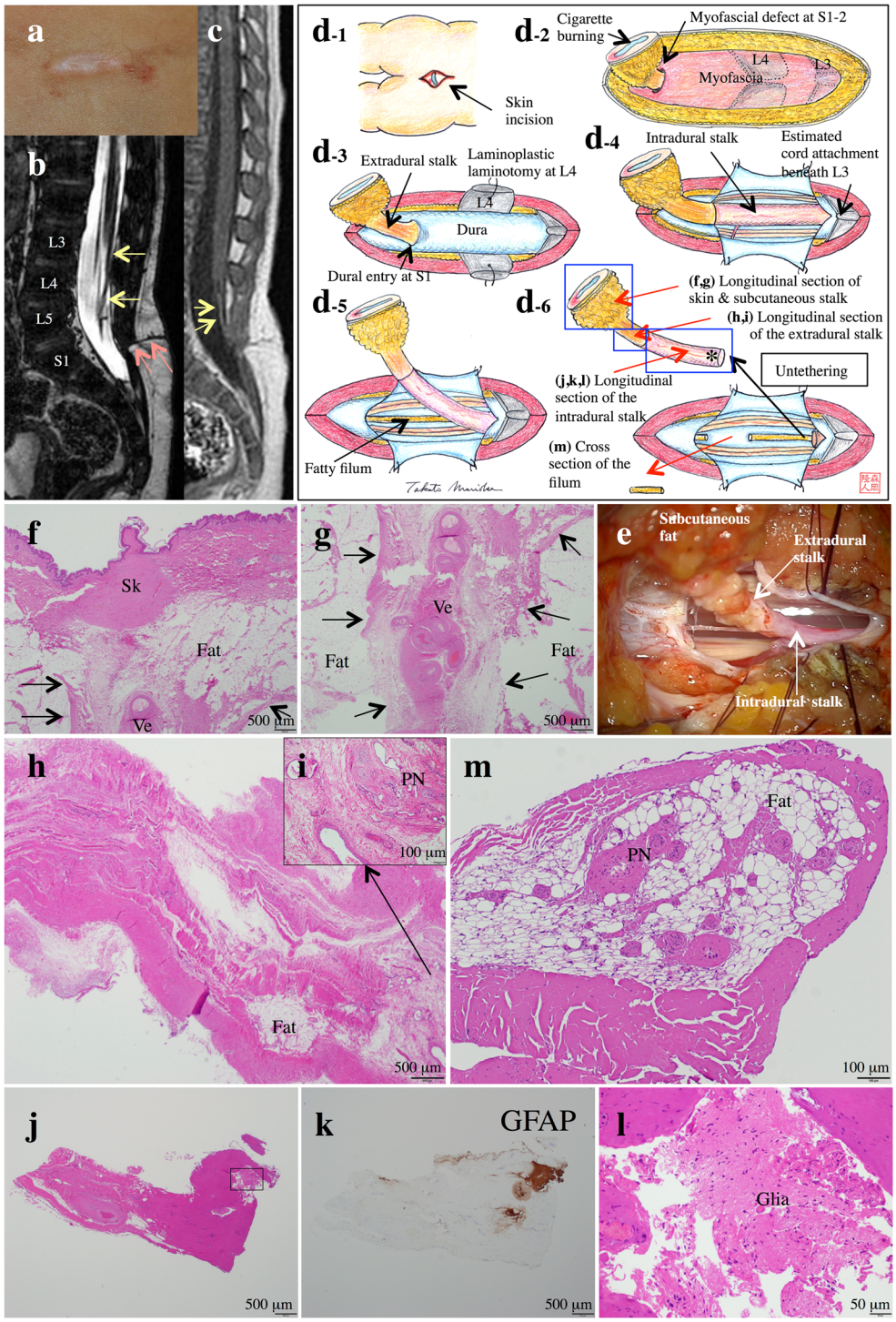


the subcutaneous region. While the fibrocollagenous stalk started beneath the skin lesion with a jagged depression of squamous epithelium in patient 2, in the remaining five patients, large amounts of adipose tissue were seen between the skin lesion and stalk (Figs. 2a, 3f, g, and 4e). Adipose tissue was also observed in the extradural stalk in patients 2 and 5 (Fig. 3h) and in the intradural stalk in patients 3 and 5. Smooth and skeletal muscle tissues were also noted in patients 3 and 4.

Associated anomalies were caudal-type lipoma and type-II split cord malformation with neurenteric cyst in patients 3 and 4, respectively, as reported previously [11]. In patient 5, filar-type lipoma was also seen (Fig. 3c, d-5, d-6, m).

◀ **Fig. 3** Patient 5 (with GFAP-immunopositive neuroglial tissues containing stalk). (*a*) Photograph showing a typical cigarette-burn skin lesion with a small angioma. (*b*) Sagittal three-dimensional-heavily T2-weighted image showing an isointense subcutaneous (red arrows) and intraspinal stalk (yellow arrows) passing through the spinal canal opposite S1 and joining the conus at L3. (*c*) Sagittal T1-weighted spoiled gradient-recalled echo image showing the high intensity of the filum (yellow arrows). (*d*) Schematic drawings and (*e*) microscopic view of the operative findings. A small elliptical skin incision is made around the skin lesion, and the stalk at the base is dissected out to the myofascial defect at S1–2 (*d-1* and *d-2*). Passage of the stalk through the dura is noted at S1 (*d-3*). Upon opening the dura, the intradural stalk is seen (*d-4*, *d-5*, *e*). Because the stalk's attachment on the cord was estimated at L3, we did not perform additional laminotomy to expose the attachment. The intradural stalk is severed at the level of L3–4 and untethering of the cord is performed (*d-6*). The proximal cut of the stalk moves to the rostral side and recedes into the spinal canal. The extra- and intradural stalk with its skin lesion is resected en bloc. (*f*, *g*) Histologically, the fibrocollagenous stalk (black arrows) containing channels of blood vessels (Ve) begins beneath the skin lesion (Sk), although a large amount of adipose tissue (Fat) lies between the skin lesion and stalk and runs into the fatty tissue. (*h*, *i*) Peripheral nerve fibers (PN) and fatty tissue are focally embedded in the extradural stalk. (*j–l*) GFAP-immunopositive neuroglial tissues (Glia) are noted in the intradural stalk near the cord attachment. The position of the GFAP-immunopositive neuroglial tissues is indicated by a black asterisk in *d-6*. (*l*) High-power image of the area indicated by the open square in *j*. (*m*) Filar tissue containing adipose tissue (Fat) and peripheral nerve fibers (PN). GFAP, glial fibrillary acidic protein

## Discussion

Although the central feature in the histopathology of an LDM stalk is the presence of neuroglial tissue in the fibrocollagenous band [16, 17], recent authors [7, 8, 11] reported that GFAP-immunopositive neuroglial tissue is not noted in every stalk. The most likely reason is that only part of the LDM stalk was subjected to histological examination [7, 8], and detailed histological examination of the entire tract is difficult in daily clinical practice [11]. In the present study, almost the entire tract of five of six patients was submitted for histological examination, although extensive examination of the entire stalk could not be performed in a strict sense. However, immunopositivity for GFAP in the stalk was observed in as few as 50% of the patients. Also, localization of GFAP-immunopositive neuroglial tissues was just caudal to the cord-stalk attachment site in two patients and in the subcutaneous lipomatous tissue in one patient [11]. No GFAP-immunopositive neuroglial tissue was observed in the most and main part of the stalk. These findings indicate that GFAP-immunopositive neuroglial tissues might not be widely distributed throughout the stalk, and detection of sparse GFAP-positive tissue is difficult with routine histopathological examination. Unlike the neuroglial tissues, peripheral nerve fibers were observed in every stalk in this study, confirming that the profuse network of peripheral nerves, with neural crest cell (NCC) origin, found in every stalk, might assist in the diagnosis of LDM [11]. Given this finding, immunohistochemical examination of S-100-expressing tissue might be useful to detect both astroglia and Schwann cells.

A notable finding in the present study is that four of the six patients had dermal melanocytosis (Mongolian spot) [3], surrounding the cigarette-burn skin lesion. In three of these four patients, histopathologically, numerous melanocytes were distributed linearly along the long axis of the intradural LDM stalk, as was seen our previous report [11]. Especially in patients 2 and 3, the intradural stalk containing high numbers of melanocytes was seen as a black color, intraoperatively [11]. Melanocytes, residing in the skin of the body, originate from trunk NCCs. According to embryonic migratory pathways, the trunk NCCs are divided into two populations: dorsally (dorsolaterally) (between surface ectoderm and somites) and ventrally (between the neural tube and somites) migrating cells. Traditionally, the dorsally migrating cells are considered the main source for melanocytes, while the ventrally migrating cells give rise to the peripheral nervous system and adrenal medulla. A recent study revealed that melanocytes migrating first ventrally also then migrate dorsally along the peripheral nerves [1]. Numerous melanocytes observed in the black-colored LDM stalks in the three patients with dermal melanocytosis might represent these migrating processes of melanocytes along the fibrocollagenous tissue and the peripheral nerves during formation of the LDM stalk. Although we saw a high incidence of melanocytes in the LDM stalks in our study, these observations were not described in Pang et al.'s original reports [16, 17]. A possible reason is racial difference, as is seen with Mongolian spots, which are most commonly seen in Asians and Africans, and less commonly in Caucasians [4].

The most frequently observed mesodermal tissue in this study, except for fibrovascular tissues, was adipose tissue, which was noted especially in the subcutaneous region. In almost all patients, large amounts of loose fatty tissue was present between the skin lesion and the stalk, indicating that there is not always a tight fibrous connection between the flat skin region and LDM stalk, as was seen in patient 3 [11]. This is an important issue during LDM stalk dissection.

Among the spinal lipomas, dorsal-type lipoma is frequently associated with LDM [16, 17]. Dorsal-type lipomas, also a pure primary neurulation defect, are thought to result from premature disjunction [12, 16, 17], while LDMs result from incomplete disjunction. Their simultaneous occurrence in the same region as a primary neural tube defect is not surprising and may represent slightly different perturbations of

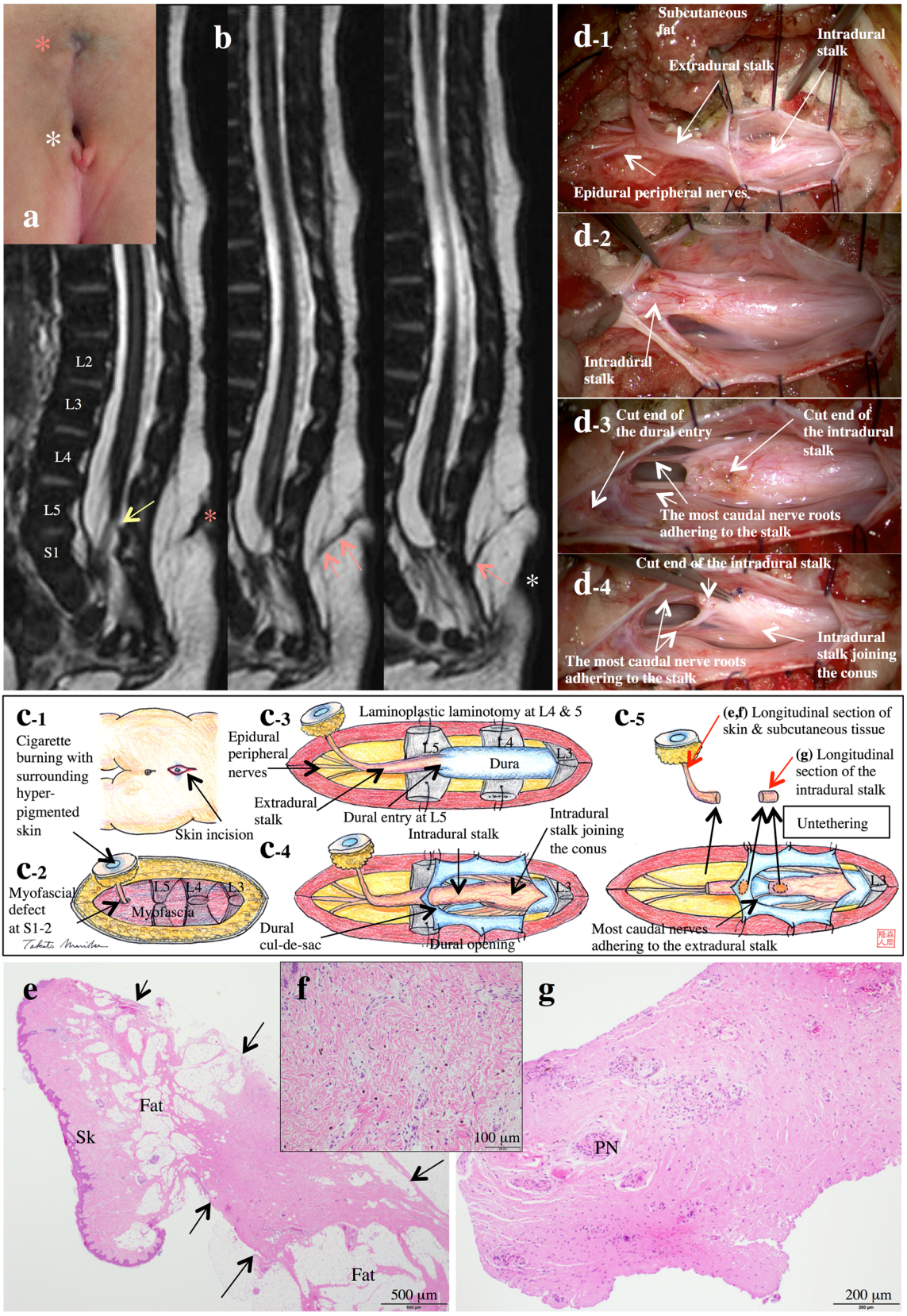
a
b
L2
L3
L4
L5
S1
d-1
Subcutaneous fat
Intradural stalk
Extradural stalk
Epidural peripheral nerves
d-2
Intradural stalk
d-3
Cut end of the dural entry
Cut end of the intradural stalk
The most caudal nerve roots adhering to the stalk
d-4
Cut end of the intradural stalk
The most caudal nerve roots adhering to the stalk
Intradural stalk joining the conus
c-1
Cigarette burning with surrounding hyper-pigmented skin
Skin incision
c-2
Myofascial defect at S1-2
Myofascia
c-3
Laminoplastic laminotomy at L4 & 5
Epidural peripheral nerves
Extradural stalk
Dural entry at L5
Dura
c-4
Intradural stalk
Intradural stalk joining the conus
Dural cul-de-sac
Dural opening
c-5
(e,f) Longitudinal section of skin & subcutaneous tissue
(g) Longitudinal section of the intradural stalk
Untethering
Most caudal nerves adhering to the extradural stalk
e
Fat
Sk
Fat
500 μm
f
100 μm
g
PN
200 μm

◀ **Fig. 4** Patient 6 (with peripheral nerve fibers containing stalk). (*a*) Photograph showing a cigarette-burn skin lesion with surrounding hyperpigmented skin, Mongolian spot (red asterisk), and a dimple with surrounding skin overhang (white asterisk). (*b*) Serial sagittal three-dimensional-heavily T2-weighted images showing a subcutaneous stalk (red arrows) beginning from the cigarette-burn skin lesion (red asterisk) and passing through the spinal canal opposite L5 to join the lower-lying conus (yellow arrow). The dimple is indicated with a white asterisk. (*c*) Schematic drawing and (*d*) microscopic view of the operative findings. A small elliptical skin incision is made around the cigarette-burn skin lesion, and the stalk at the base is dissected out to the myofascial defect at S1–2 (*c-1* and *c-2*). Passage of the stalk through the dura is noted at L5 (*c-3*). Upon opening the dura, the intradural stalk is seen (*c-4*, *d-1*, and *d-2*). Although the stalk's attachment on the lower-lying cord is confirmed at L4, most caudal nerve roots are adhered to the ventral aspect of the intradural stalk. Resection of the most caudal part of the intradural stalk and untethering of the cord are performed (*c-5*, *d-3*, and *d-4*). The extradural stalk, except for the dural entry section, with its skin lesion, is resected. (*e*) Histologically, the epidural fibrocollagenous stalk (black arrows) containing a large amount of adipose tissue (Fat) begins beneath the skin lesion (Sk). (*f*) Skin tissue showing an increased number of melanocytes. (*g*) The intradural stalk is also a fibrocollagenous tract containing peripheral nerve fibers (PN)

disjunction caused by the same insult in the same spot or in neighboring loci [16, 17]. However, in the present study, the associated spinal lipomas were caudal- and filar-type lipomas, which are thought to be a secondary neurulation defect [12]. Although an anatomical relationship between the filar-type lipoma, conus, and the LDM stalk was not confirmed in patient 5, the intradural LDM stalk joined the dorsal surface of the cord above the conus in a neighboring locus to the caudal-type lipoma in patient 3 [11], suggesting that an association with these lipomas was probably not coincidental. The development of this rare combination likely occurs during the critical transition between the end of primary, and the beginning of secondary, neurulation, in a stage aptly called junctional neurulation [2].

In conclusion, GFAP immunopositivity in neuroglial tissue in the LDM stalk was seen in only 50% of our patients despite the relatively extensive histopathological examination. We confirm that the clinical diagnosis of LDM should be based on comprehensive examination of histopathological findings as well as clinical manifestations [11]. The profuse network of peripheral nerve fibers in every stalk and the high incidence of melanocyte accumulation associated with dermal melanocytosis might assist in the histopathological diagnosis of LDM because both tissues are of NCC origin.

**Acknowledgments** We thank Jane Charbonneau, DVM, from Edanz Group (www.edanzediting.com/ac) for editing a draft of this manuscript.

**Funding information** This work was partly supported by the Research Foundation of Fukuoka Children's Hospital.

## Compliance with ethical standards

**Conflict of interest** The authors declare that they have no conflict of interest.

## References

1. Cichorek M, Wachulska M, Stasiewicz A, Tyminska A (2013) Skin melanocytes: biology and development. Postepy Dermatol Alergol 1:30–41
2. Eibach S, Moes G, Hou YJ, Zovickian J, Pang D (2017) Unjoined primary and secondary neural tubes: junctional neural tube defect, a new form of spinal dysraphism caused by disturbance of junctional neurulation. Childs Nerv Syst 33:1633–1647
3. Franceschini D, Dinulos JG (2015) Dermal melanocytesis and associated disorders. Curr Opin Pediatr 27:480–485
4. Gupta D, Thappa DM (2013) Mongolian spots: how important are they? World J Clin Cases 16:230–232
5. Hashiguchi K, Morioka T, Fukui K, Miyagi Y, Mihara F, Yoshiura T, Nagata S, Sasaki T (2005) Usefulness of constructive interference in steady-state (CISS) MR imaging in the presurgical examination for lumbosacral lipoma. J Neurosurg (6 Pediatrics) 103:537–543
6. Hashiguchi K, Morioka T, Yoshida F, Miyagi Y, Mihara F, Yoshiura T, Nagata S, Sasaki T (2007) Feasibility and limitation of constructive interference in steady-state (CISS) MR imaging in neonates with lumbosacral myeloschisis. Neuroradiology 49:579–585
7. Lee JY, Chong S, Choi YH, Phi JH, Cheon J-E, Kim S-K, Park SH, Kim I-O, Wang K-C (2017) Modification of surgical procedure for "probable" limited dorsal myeloschisis. J Neurosurg Pediatr 19:616–619
8. Lee JY, Park S-H, Chong S, Phi JH, Kim S-K, Cho B-K, Wang K-C (2018) Congenital dermal sinus and limited dorsal myeloschisis: "spectrum disorders" of incomplete dysjunction between cutaneous and neural ectoderms. Neurosurgery (Epub ahead of print)
9. Morioka T, Hashiguchi K, Yoshida F, Nagata S, Miyagi Y, Mihara F, Sasaki T (2007) Dynamic morphological changes in lumbosacral lipoma during the first months of life revealed by constructive interference in steady-state (CISS) MR imaging. Childs Nerv Syst 23:415–420
10. Morioka T, Murakami N, Shimogawa T, Mukae N, Hashiguchi K, Suzuki SO, Iihara K (2017) Neurosurgical management and pathology of lumbosacral lipomas with tethered cord. Neuropathology 37:385–392
11. Morioka T, Suzuki SO, Murakami N, Shimogawa T, Mukae N, Inoha S, Sasaguri T, Iihara K (2018) Neurosurgical pathology of limited dorsal myeloschisis. Childs Nerv Syst 34:293–303
12. Morota N, Ihara S, Ogiwara H (2017) New classification of spinal lipomas based on embryonic stage. J Neurosurg Pediatr 19:428–439
13. Murakami N, Morioka T, Hashiguchi K, Yoshiura T, Hiwatashi K, Suzuki SO, Nakamizo A, Amano T, Hata N, Sasaki T (2013) Usefulness of three-dimensional T1-weighted spoiled gradient-recalled echo and three-dimensional heavily T2-weighted images in preoperative evaluation of spinal dysraphism. Childs Nerv Syst 29:1905–1914
14. Murakami N, Morioka T, Ichiyama M, Nakamura R, Kawamura N (2017) Lateral lipomyelomenigocele of the hemicord with split cord

malformation type I revealed by 3D heavily T2-weighted MR imaging. Childs Nerv Syst 33:993–997
15. Murakami N, Morioka T, Shimogawa T, Hashiguchi K, Mukae N, Uchihashi K, Suzuki SO, Iihara K (2018) Retained medullary cord extending to a sacral subcutaneous menigocele. Childs Nerv Syst 34(3):527–533
16. Pang D, Zovickian J, Oviedo A, Moes GS (2010) Limited dorsal myeloschisis: a distinctive clinicopathological entity. Neurosurgery 67:1555–1580
17. Pang D, Zovickian J, Wong S-T, Hou YJ, Moes GS (2013) Limited dorsal myeloschisis: a not-so-rare form of primary neurulation defect. Childs Nerv Syst 29:1459–1484
18. Shirozu N, Morioka T, Inoha S, Imamoto N, Sasaguri T (2018) Enlargement of sacral subcutaneous meningocele associated with retained medullary cord. Childs Nerv Syst (Epub ahead of print)